Life Sciences 194 (2018) 104–110

Contents lists available at ScienceDirect

Life Sciences

journal homepage: www.elsevier.com/locate/lifescie

Transferrin targeted liposomal 5-fluorouracil induced apoptosis *via* mitochondria signaling pathway in cancer cells

Eskandar Moghimipour[a,b], Mohsen Rezaei[c], Zahra Ramezani[a], Maryam Kouchak[a], Mohsen Amini[d], Kambiz Ahmadi Angali[e], Farid Abedin Dorkoosh[f,g], Somayeh Handali[a,*]

[a] Nanotechnology Research Center, Ahvaz Jundishapur University of Medical Sciences, Ahvaz, Iran
[b] Cellular and Molecular Research Center, Ahvaz Jundishapur University of Medical Sciences, Ahvaz, Iran
[c] Department of Toxicology, Faculty of Medical Sciences, Tarbiat Modares University, Tehran, Iran
[d] Department of Medicinal Chemistry, Faculty of Pharmacy, Tehran University of Medical Sciences, Tehran, Iran
[e] Department of Biostatistics, School of Public Health, Ahvaz Jundishapur University of Medical Sciences, Ahvaz, Iran
[f] Department of Pharmaceutics, Faculty of Pharmacy, Tehran University of Medical Sciences, Tehran, Iran
[g] Medical Biomaterial Research Centre (MBRC), Tehran University of Medical Sciences, Tehran, Iran

ARTICLE INFO

Keywords:
5-Fluorouracil
Liposome
Transferrin
Cancer
Apoptosis

ABSTRACT

The purpose of this study was to prepare transferrin (Tf) targeted liposomal 5-Fluorouracil (5FU) to improve the safety and efficacy of the drug. Liposomes were prepared using thin layer method. Morphology of liposomes was characterized by transmission electron microscopy (TEM) and their particle size was also determined. The *in vitro* cytotoxicity was investigated *via* MTT assay on HT-29 (as cancer cell) and fibroblast (as normal cell). Moreover, cytotoxicity mechanism of targeted liposomes was determined through the production of reactive oxygen species (ROS), mitochondrial membrane potential ($\Delta\Psi_m$) and release of cytochrome *c*. Results showed that encapsulation efficiency (EE%) was 58.66 ± 0.58 and average size of liposomes was 107 nm. Also, nanoparticles were spherical as shown by TEM. MTT assay on HT-29 cells revealed the higher cytotoxic activity of targeted liposomes in comparison to free drug and non-targeted liposome. In contrast, comparing with cancer cells, targeted liposomes had no cytotoxic effect on normal cells. In addition, targeted liposomes induced apoptosis through activation of mitochondrial apoptosis pathways, as evidenced by decreased mitochondrial membrane potential and release of cytochrome *c*. Results of the study indicated that targeted liposomes would provide a potential strategy to treat colon cancer by inducing apoptosis *via* mitochondria signaling pathway with reducing dose of the drug and resulting fewer side-effects.

1. Introduction

Colon cancer is a major cause of morbidity in the world. 5FU is the first-line treatment against colon cancer for many years [1]. Due to structural similarity to the pyrimidine base of DNA and RNA, 5FU interferes with nucleoside metabolism, leading to cytotoxicity and cell death [2]. However, clinical applications of 5FU has drawbacks including short half-life (20 min) due to rapid metabolism and non-specific drug distribution resulting sever systemic toxicity on bone marrow cells, gastrointestinal tract, hematological, neural, cardiac and dermatological effects [2–4]. Therefore, several approaches have been attempted to improve the delivery of 5FU in order to enhance therapeutic index with reducing side effects. Encapsulation of 5FU in nanoparticles, such as liposomes, can decrease drug clearance and reduce its associated toxicity [5]. Liposomes are sphere-shaped vesicles composed of one or more phospholipid bilayers [6]. They are considered as efficient drug delivery system for drugs with different physicochemical properties, diagnostics, vaccines and other bio-molecules [6]. As drug delivery, liposomes have many advantages such as biodegradability, biocompatibility, nontoxic properties, ability to encapsulate both hydrophilic and lipophilic drugs and providing the protection of drugs from the external micro environment [7,8]. In order to improve liposomal drug delivery to the tumor site, targeting approaches with the conjugation of ligands to the surface of liposomes have been extensively studied. Targeted drug delivery improves the therapeutic effect of drugs by increasing circulation half-life, reduction of toxic side effects and allowing higher specificity in the delivery of the drug to the tumor cells [9]. Transferrin, a 78 kDa-monomeric glycoprotein responsible for cellular iron absorption, is one such molecule that can be employed for targeting [10]. The Tf receptor (TfR) is overexpressed in 90% of tumors

* Corresponding author.
E-mail address: handali_s81@yahoo.com (S. Handali).

https://doi.org/10.1016/j.lfs.2017.12.026
Received 3 October 2017; Received in revised form 16 December 2017; Accepted 20 December 2017
Available online 21 December 2017
0024-3205/

[7] and high specificity of endocytosis uptake of Tf by the TfR has further made it a subject of interest for targeted drug delivery [11].

Molecular mechanisms of many cytotoxic chemotherapeutic agents are known. There are various patterns of cell death when the cells are exposed to anticancer drugs. Many cell death-associated signal transduction pathways are promoted through mitochondrial function [12]. Apoptosis or programmed cell death plays a critical role in response to stress-induced or certain regulatory signals. There are two main apoptotic pathways: the intrinsic or mitochondrial pathway and the extrinsic or death receptor pathway. The intrinsic apoptotic pathway is activated by various intracellular stimuli, including DNA damage, oxidative stress and growth factor deprivation. The extrinsic pathway of apoptosis is initiated by the binding of death ligands such as Fas ligand and TNF-α to death receptors of the TNF receptor super family [13]. Reactive oxygen species (ROS) is one of the main factors related to the cell death. The value of ROS may determine the selection between necrosis and apoptosis [14]. It has been reported that low and high levels of ROS regulate apoptotic and necrotic signaling pathway, respectively [15]. The apoptotic pathway induction is a desirable end point when treating the cancer since it will not induce inflammation. Targeting formulation is focused on improvement of agents that selectively inhibit the growth of cancer cells with reducing toxicity while maintaining a therapeutic window. This approach might improve the efficacy of anticancer agents by affecting the mitochondria and trigger cell death pathway in different ways from traditional chemotherapy which can emerge as a promising means to cancer therapy.

The objective of the present study was to prepare and characterize 5FU loaded transferrin targeted liposome. In addition, we evaluated the potential of targeted liposomes to selectively deliver of the drug to cancer cell and we further investigated the mechanism of cell death.

2. Material and methods

5FU and soya phosphatidyl choline (PC) were purchased from Acros, USA. Distearoylphosphatidylethanolamine (DSPE) was obtained from Lipoid, Germany. Cholesterol, succinic anhydride and *N*-hydroxysuccinimide (NHS) were acquired from Merck, Germany. 1-Ethyl-3-(3-dimethylaminopropyl) carbodiimide (EDC) was purchased from Alfa Aesar, Germany. Tf was obtained from Sigma-Aldrich, Germany. Metronidazole was kindly donated by Pars Darou Pharmaceutical Co., Iran.

HT-29 (human colorectal adenocarcinoma) and fibroblast (Hu02) cells were obtained from Iranian Biological Resource Center (IBRC). Dulbecco's modified eagle's medium (DMEM) and fetal bovine serum (FBS) were purchased from Gibco, USA. Penicillin-streptomycin and 5-diphenyl tetrazolium bromide (MTT) were acquired from Sigma-Aldrich, Germany. 2′,7′-Dichlorofluorescin diacetate (DCFDA) was obtained from Sigma-Aldrich, Germany. MitoLight™ Apoptosis Detection kit was provided from Merck Millipore, USA. Cytochrome c human ELISA kit was purchased from Abcam, USA and Annexin V-FITC apoptosis detection kit was acquired from Sigma Aldrich, USA. All of the solvents were of the analytical grade.

2.1. Synthesis of Tf-DSPE

The schematic of synthesis of Tf-DSPE was carried out as shown in Fig. 1. The conjugation of Tf to DSPE was performed in two steps. Firstly, DSPE (200 mg, 0.27 mmol) was dissolved in 20 mL of dry chloroform. Then succinic anhydride (200 mg, 2 mmol) was added and stirred at room temperature for 48 h. Thereafter, 100 mL chloroform and 20 mL deionized water added under stirring and this mixture was incubated for 30 min. This procedure was repeated twice and then the chloroform layer was separated. To remove the traces of water present in separated chloroform layer, it was treated with anhydrous sodium sulphate and chloroform was evaporated using rotary evaporation (Heidolph, Germany). In the second step, activated-DSPE (10 mg) was dissolved in 5 mL of dimethyl sulfoxide (DMSO). Afterward, EDC (500 mg) and NHS (400 mg) were added and the mixture was incubated at room temperature for 6 h. The aqueous solution of transferrin (10 mg/mL) was added under stirring at room temperature for 24 h. The resulting solution was diluted with deionized water and dialyzed twice against deionized water using dialysis membrane (MWCO 12 kDa) and finally freeze-dried to get dry powder (Operon, Korea). Conjugates were characterized by Fourier transform infrared spectroscopy (FT-IR) (Perkin-Elmer, USA).

2.2. Preparation of liposomes

Liposomes were prepared using thin film hydration method. Briefly, PC/cholesterol/Tf-DSPE at different molar ratio of 0.5:1:0.0061, 1:1:0.0061 and 2:1:0.0061 were dissolved in chloroform in a round bottom flask. The thin lipid film was formed by removing chloroform under rotary evaporation. Lipid film was hydrated with phosphate buffer saline (PBS, pH 7.4) containing 5FU (1.5 mg) by sonication in a water bath for 15 min. Then, the suspension was homogenized for another 5 min. The non-encapsulated 5FU was separated by centrifugation at 15,000 rpm for 30 min (MPW-350R, Poland). The resulted formulation was lyophilized and stored at 4 °C for further analysis.

2.3. Determination of encapsulation efficiency

Determination of 5FU loaded in liposomes was performed using high performance liquid chromatography (HPLC) system (Waters, USA). The analysis was carried out on C_{18} column (250 × 4 mm i.d., 5 μm) at 30 °C and the wavelength was set at 260 nm. The mobile phase was consisted of 0.02 M phosphate buffer pH 4 and methanol (70:30, V/V) at a flow rate 0.8 mL/min. Injection volume was 50 μL and metronidazole was used as internal standard. The encapsulation efficiency (EE%) was determined in accordance with Eq. (1):

$$EE\% = (A_I - A_F/A_I) \times 100 \quad (1)$$

where, A_I is the amount of 5FU initially added to the formulation and A_F is the amount of the free drug in the supernatant after centrifugation [4].

2.4. Morphology study and particle size of liposomes

Morphology of liposomes was determined by transmission electron microscopy (TEM, LEO 906, Zeiss, Germany). Samples were first dispersed in deionized water and then one drop of the suspension was placed onto a carbon-coated copper TEM grid. Particle size of liposomes was also analyzed using a particle sizer (Qudix, Scatteroscope I system, Korea) at 25 °C. Samples were diluted with deionized water and sonicated prior to measurement.

2.5. Cytotoxicity assay

In vitro cytotoxicity activity was evaluated using MTT method based on the cleavage of yellow tetrazolium salt MTT by metabolically active cells to form a dark purple formazan dye [16,17]. HT-29 (colon cancer cell line) and fibroblast (normal cell) were grown at 37 °C, 5% CO_2 and 95% relative humidity in DMEM supplemented with 10% FBS and 1% penicillin-streptomycin. Cells was seeded at a density of 1×10^4 in 96-well plates and were incubated for 24 h. Supernatants from the wells were aspirated out and replaced with fresh growth medium containing different concentrations of 5FU, liposomal 5FU and Tf-liposomal 5FU (25, 35, 50, 75 and 100 μM) for 48 h. At the end of incubation time, 20 μL of MTT (5 mg/mL in PBS) solution was added into each well and incubated at 37 °C for another 4 h. Then, DMSO (150 μL) was added in each well and the plates were placed on a plate shaker for 20 min. The absorbance of each plate was read at 570 nm using ELISA plate reader (BioRad, USA). Cellular viability was determined using the Eq. (2) and

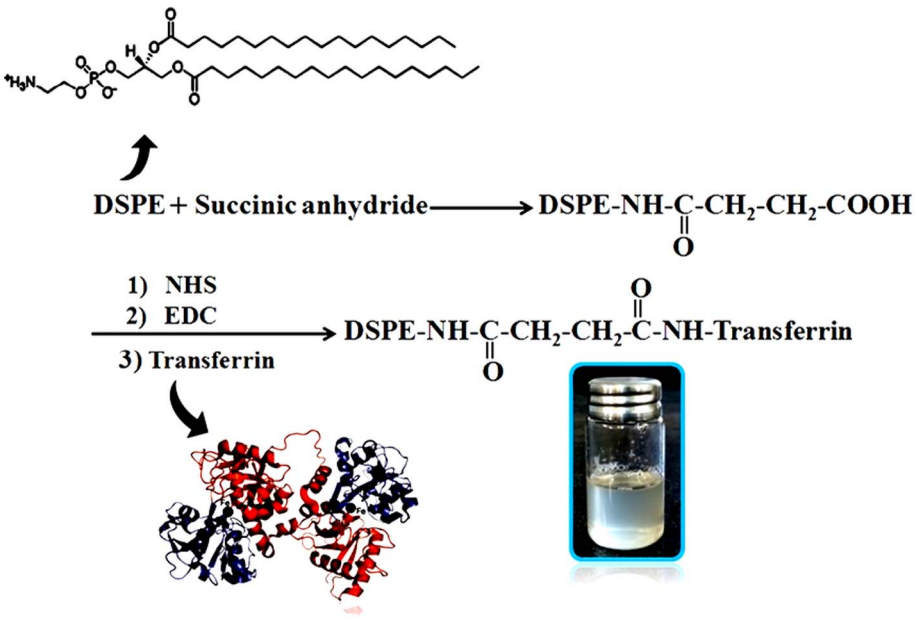

Fig. 1. Synthesis schematic of Tf-DSPE.

the half maximal inhibitory concentration (IC_{50}) was calculated as cytotoxicity parameter.

$$\text{Cell viability\%} = (Abs_{sample}/Abs_{control}) \times 100 \quad (2)$$

It should be noted that based on MTT studies, no significant differences in cell viability were found between 5FU and liposomal 5FU in cancer cells. Therefore additional investigations as mentioned below were only performed for 5FU and Tf-liposomal 5FU at their IC_{50} concentrations.

2.6. Measurement of reactive oxygen species (ROS)

ROS production in cells was measured using 2′,7′-dichlorofluorescin diacetate (DCFDA). In briefly, DCFDA diffuses into cells and is deacetylates by cellular esterases to non-fluorescent compound which oxidizes by intracellular ROS into fluorescent 2′,7′-dichlorodihydrofluorescein (DCF) [18]. Cells at a density of 1×10^5 were seeded into 6-well plate for 24 h. Then cells were incubated with free 5FU and Tf-liposomal 5FU for 1, 3 and 48 h. At the end of the incubation period, cells were washed with PBS and exposed with 10 μM DCFDA for 45 min at 37 °C. Fluorescence was detected at excitation wavelength of 485 nm and emission wavelength of 530 nm using spectrofluorimeter (PerkinElmer, USA).

2.7. Mitochondrial transmembrane potential ($\Delta\Psi_m$) analysis

Change in $\Delta\Psi_m$ was detected by MitoLight™ apoptosis detection kit (Merck Millipore, USA). Briefly, cells at a density of 1×10^5 were seeded into 6-well plate for 24 h. Then cells were treated with 5FU and Tf-liposomal 5FU for 48 h. After incubation time, they were exposed to MitoLight™ solution and incubated for 15–20 min at 37 °C. Cells were centrifuged and re-suspended in incubation buffer and analyzed using flow cytometer (Facs Calibur, BD, USA).

2.8. Release of cytochrome c from mitochondria

Detection of cytochrome *c* released from the mitochondria to the cytoplasm was carried out using cytochrome *c* human ELISA kit according to the manufacturer's instructions (Abcam, USA). Cells were exposed with 5FU and Tf-liposomal 5FU for 48 h. 100 μL of samples were added to the microplates and 50 μL of biotin conjugated antibody was added to each well and incubated at room temperature (18 to 25 °C) for 2 h. 100 μL of streptavidin-HRP was added to all wells and incubated at room temperature for 1 h. Then 100 μL of TMB solution was pipetted into each well. When a dark blue color was observed, the enzyme reaction was stopped by adding 100 μL of stop solution and cytochrome *c* release was determined by measuring absorbance at 450 nm using an ELISA plate reader (BioRad, USA).

2.9. Determination of apoptosis

To assess the rate of apoptosis, Annexin V-FITC apoptosis detection kit was used according to the manufacturer's protocol (Sigma Aldrich, USA). Briefly, cells were seeded into 6-well plates (1×10^6 cells/well) for 24 h. Then they were exposed to 5FU and Tf-liposomal 5FU for 48 h. After the incubation, cells were collected and re-suspended in binding buffer and 5 μL of Annexin V-FITC and 10 μL of Propidium Iodide (PI) were added. The samples were incubated at room temperature for 10 min and protected from light. The apoptosis rates were measured using a flow cytometer (Facs Calibur, BD, USA).

2.10. Statistical analysis

All data were presented as mean values ± SD. Statistical comparisons among groups were performed by one-way analysis of variance (ANOVA) and $p < 0.05$ was considered statistically significant. Each experiment was repeated at least for three independent times. Normality of data was performed by Kolmogorov-Smirnov test at $\alpha = 0.5$ (p-value > 0.05) and normality ascertained. Homogeneity of variance was performed by Levene test at $\alpha = 0.5$. F-ANOVA was used when homogeneity of variances was established and Welch test was utilized to evaluate the non-homogeneity variances of groups.

3. Results and discussion

3.1. Synthesis and characterization of Tf-DSPE

The conjugate structure was confirmed by FTIR spectroscopy as shown in Fig. 2. The spectrum of activated-DSPE showed an ester, carboxylic acid and amide C═O stretching vibrations at 1737, 1713 and 1650 cm^{-1}, respectively. The absorption bands at 1540 cm^{-1} belong to the N—H bending vibration of amide bond. The absorption bands at 3100–3500 attributed to symmetric —N—H stretching vibrations. Antisymmetric and symmetric stretching vibrations of aliphatic

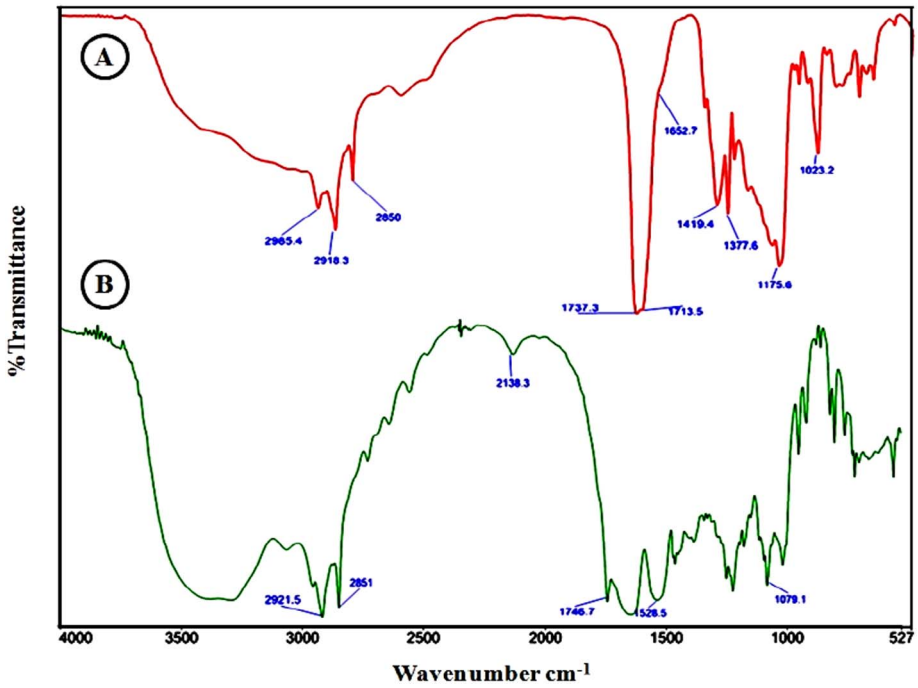

Fig. 2. The FTIR spectrum A) activated-DSPE and B) Tf-DSPE.

C−H groups are corresponding to the bands at 2918 and 2850 cm^{-1}. Moreover, the peaks related to the O = P−OH stretching vibrations and P═O group in DSPE appeared at 2550–2700 cm^{-1} and 1100–1200 cm^{-1}, respectively.

The presence of amide bonds is the main feature of all biological samples. As it was shown in Fig. 2B, two prominent amide absorption bands were found at 1540 cm^{-1} for N−H bending vibrations and around 1650 cm^{-1} for C═O stretching vibrations. The strong peak at 3200–3400 cm^{-1} superposed with the broad, overlapped −OH stretching vibrations was attributed to N−H stretching vibration of the peptide bonds in transferrin.

3.2. Characterization of the liposomes

The efficiency of drug encapsulation in liposomes at different molar ratios PC to cholesterol; 0.5:1, 1:1 and 2:1 were 20.61 ± 1.88, 30.19 ± 1.10 and 58.66 ± 0.58, respectively. According to the results, by encasement the amount of PC, encapsulation efficiency was increased. The present findings are consistent with other research which found that 5FU entrapment efficiency can be increased by increasing the amount of phospholipids [19,20]. It was reported that by increasing the amount of phospholipids, liposomes become more rigid with ability to retain more drugs [21]. Moreover, high lipid content leads to a significantly increased ratio of aqueous volume within the vesicles in comparison with the surrounding aqueous volume [22]. Because the encapsulation efficiency of polar drugs is associated with the quantity of aqueous phase that is immobilized between the phospholipid bilayers and the concentration of the drug in the aqueous phase [20]. Particle size distribution and TEM image of liposomes are shown in Fig. 3A and B. According to previous reports, nano-particles with particle size of 100 to 200 nm can accumulate in solid tumors by enhanced permeability and retention (EPR) effects due to presence of leaky blood vessels and defective lymphatic drainage [23]. In addition, in order to internalize of nano-particles into cells, their size should be large enough to prevent rapid leakage into blood capillaries, but small enough to escape from macrophages that are lodged in the reticuloendothelial system (RES). For this purpose, the mean size of nano-particle in the range of 100–400 nm is preferred [24]. In our study, the mean particle size of liposomes was around to be 107 nm, which would be considered favorable for internalization into targeted cells. The morphology of liposomes was evaluated by TEM. According to the Fig. 3B, liposomes were spherical in shape without any aggregation or fusion.

3.3. Evaluation of cytotoxic activity

The cytotoxicity of 5FU, liposomal 5FU and Tf-liposomal 5FU was determined by MTT assay that is based on the ability of mitochondrial succinic dehydrogenase enzyme of living cell to convert the yellow dye MTT to dark purple formazan dye [16]. Here, HT-29 cells were selected as colon cancer cell lines and fibroblast cells also were used as normal cells in order to find out whether targeted liposome has any cytotoxic effect on normal cells. Various concentrations of agents were considered for MTT assay based on our previous studies. As it could be seen from Fig. 4, Tf-liposomal 5FU showed higher cytotoxicity than 5FU and liposomal 5FU in cancer cells through a dose-dependent manner ($p < 0.05$). The IC_{50} values for 5FU, liposomal 5FU and Tf-liposomal 5FU were 66.069, 58.88 and 31.62 μM, respectively. Also, as seen in the Fig. 4, no significant difference was found between cytotoxicity of 5FU and liposomal 5FU that may be due to impeded internalization of non-targeted liposomes in the cells [25]. This finding indicated that targeted liposomal formulations with Tf was not only modified the cellular uptake of the liposomes but also resulting in the achievement of better therapeutic effect with further reduction in dose of 5FU. This finding confirms previous research of Sun et al. [25]. They reported that Tf targeted micelles showed higher cytotoxicity on K562 cancer cells. The cytotoxic activity of targeted nano-particles was attributed to the transferrin-receptor mediated cellular uptake and as results higher nano-particles internalization [25]. The similar result is also found in the investigation of Zhang et al. [26]. They expressed that targeted nano-particles could efficiently promote cellular uptake of artesunate and subsequently increase drug intracellular accumulation in MCF-7 cancer cells. They suggested that this uptake was probably due to TfR is highly expressed on cancer cells surface which resulting in rapid uptake of nano-particles into tumor cells *via* receptor-mediated endocytosis [26]. These results further support the idea of Singh et al. [27]. They demonstrated that the higher cytotoxicity effect of Tf targeted docetaxel loaded nano-particles on A549 cells is due to transferrin receptor

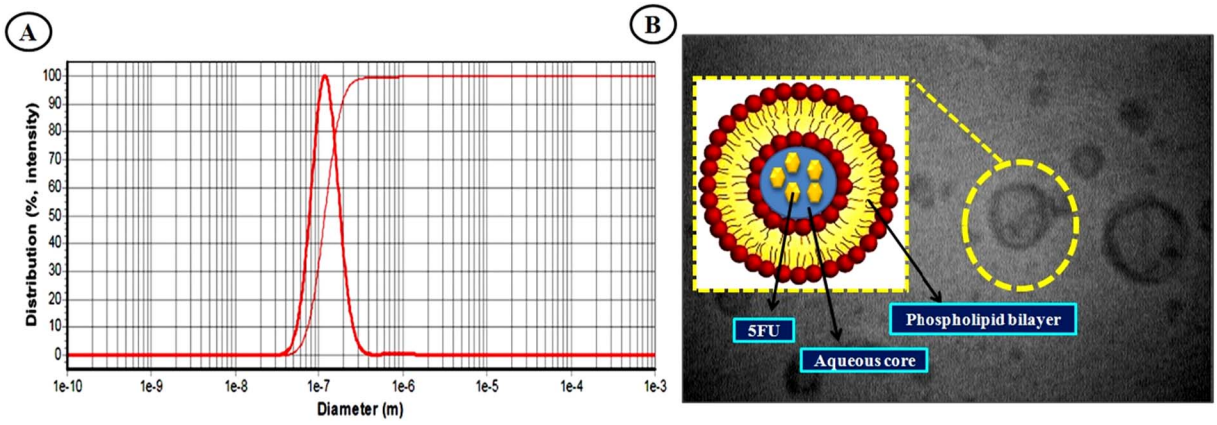

Fig. 3. A) Particle size distribution and B) TEM image of liposomes.

mediated endocytosis mechanism [27].

A remarkable finding (Fig. 4B) was that cytotoxicity of liposomal 5FU and Tf-liposomal 5FU in fibroblast cells was lower than free drug, because the expression of TfR is higher in tumor cells as compared with normal cells [28]. The aim of cancer therapy is to promote the death of cancer cells without damaging normal cells [29]. Our results confirm the finding that the targeting of liposome improves cytotoxic activity of drug toward cancer cell with lower cytotoxicity on normal cells. Our results are also accordant with finding of Kim et al. [30]. They used L929 cell as normal cells for efficacy of doxorubicin loaded Tf targeted nano-particles. They observed that targeting nano-particles were prevented the cellular uptake of drug on L929 cells because L929 cells had not Tf receptors. On the other hands, the anticancer activity of the drug in targeted nano-particles was improved than free doxorubicin in HCT 116 and KB cells as cancer cells [30]. Huang et al. [31] indicated that toxicity of Tf targeted selenium nano-particles toward HUVEC human normal cells was much lower than its toxicity in cancer cells [31].

3.4. Cytotoxicity pathway evaluation in HT-29 cells exposed to IC_{50} concentrations of 5FU and Tf-liposomal 5FU

According to the results of previous studies, many chemotherapeutic agents trigger apoptosis and necrosis based on overproduction of ROS to toxic level for creating the lethal effects in cancer cells [15,32]. According to previous report, 5FU trigger its cytotoxicity by increasing the intracellular ROS level [33]. As shown in Fig. 5A, following exposure HT-29 cells to 5FU and Tf-liposomal 5FU, 5FU displayed a higher intracellular ROS generation. The mitochondrial electron-transport chain is the major site of ROS [34], so anticancer drug may damage electron transport chain and result leakage of ROS in cancer cell. Conversely, overproduction of ROS can induce mitochondrial damage and ultimately causes cell death [35]. In view of the fact that the mitochondrial membrane potential ($\Delta\psi_m$) drops significantly followed by ROS generation, we measured potential changes of $\Delta\psi_m$ in cancer cells. Changes in $\Delta\psi_m$ were determined using MitoLight dye. Cells with high $\Delta\psi_m$ were indicated by red fluorescence (derived from aggregates), while cells with depolarized mitochondria produced green fluorescence (derived from monomers) [36]. As displayed in Fig. 5B, the $\Delta\Psi_m$ of HT-29 cells treated with free drug and Tf-liposome 5FU was 0.18% and 6.36%, respectively. The results implied that after applying targeted liposomes the cells had the biggest dissipation of $\Delta\Psi_m$. Destruction of $\Delta\Psi_m$ leads to the release of cytochrome *c* from mitochondria to cytosol which is a key initiator in the mitochondrial apoptosis pathway [37]. A remarkable release of cytochrome *c* was found in the cells that exposed to targeted drug liposome (Fig. 5C). The finding is consistent with the results for mitochondria depolarization and cell apoptosis. On the other hand, we measured the activity of caspase 3/7, which gives an accurate estimate of the cell death in the face of 5FU. According to the results, increased the activity of this enzyme was in parallel of the increased rate of apoptosis. Therefore, we did not measure the activity of these enzymes for targeted liposomes. Previous studies indicated that low levels of ROS regulate apoptotic signaling pathway, while high levels are regarded as being responsible for necrotic pathway [15]. Because apoptosis will not induce inflammation and is a favorite target of many treatment strategies, it is considered more favorable than necrosis [38]. Regarding the Fig. 5D, it was observed that Tf-liposomal 5FU induced a higher rate of apoptosis on cancer cell compared with free drug. On the other hand, it should be noted that targeted liposomes exhibit higher apoptosis with lower IC_{50}: 31.62 μM in comparison of free drug with IC_{50}: 66.069 μM. The results of this study indicated that targeting liposomal 5FU with Tf enhanced its potency by an additive action on cytotoxicity at lower concentration that in turn would reduce the side effects associated with the drug. The findings of the current study are in agreement with Szwed et al. results

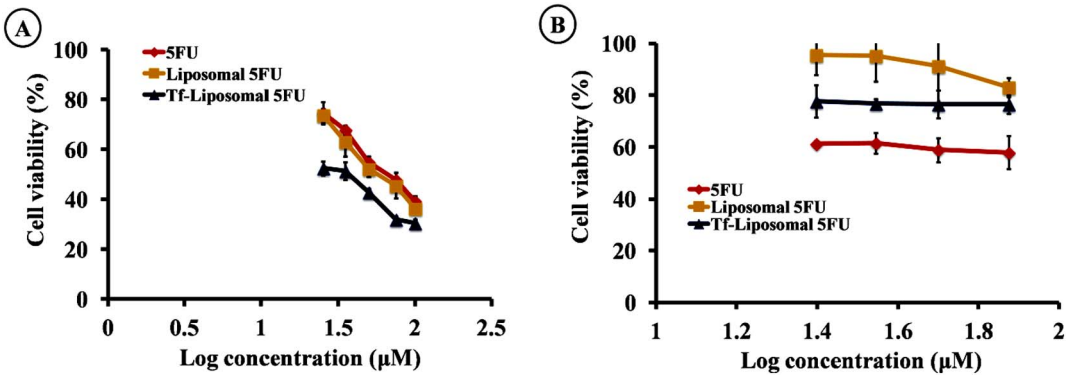

Fig. 4. Cytotoxicity of different formulations of 5FU on A) HT-29 and B) fibroblasts by MTT method in DMEM medium at 37 °C for 48 h.

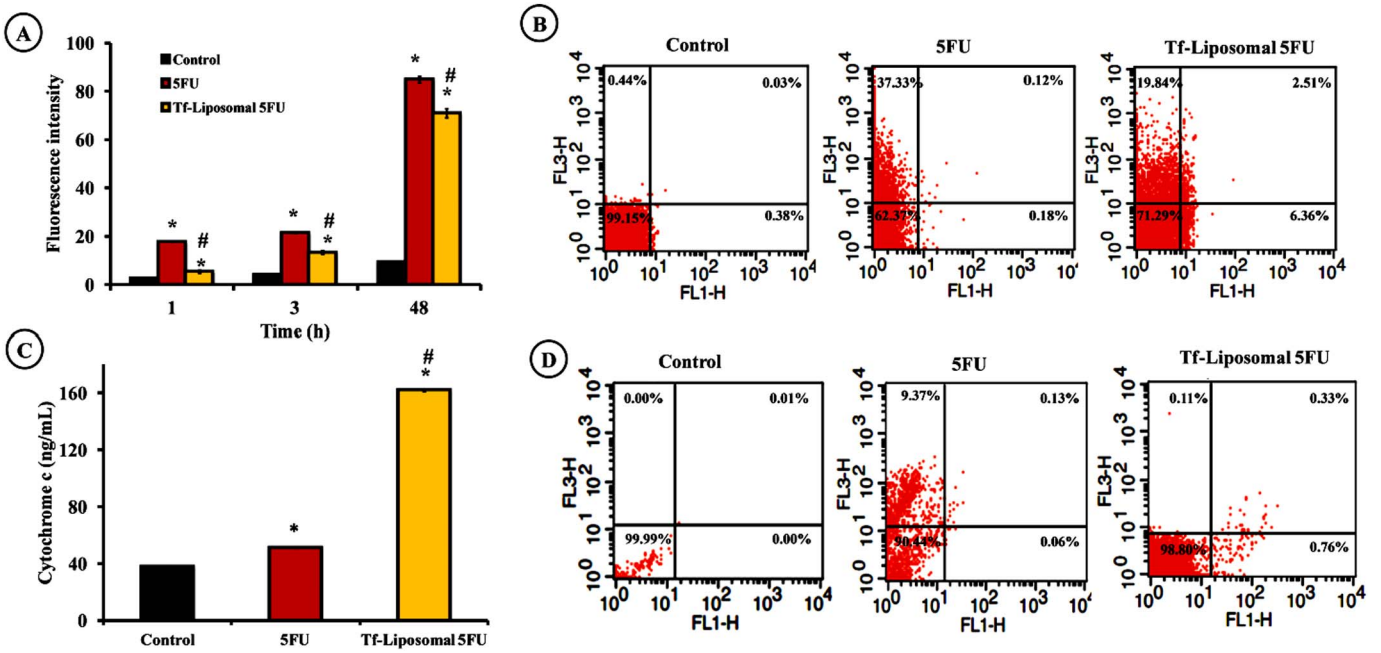

Fig. 5. The intracellular effects of free 5FU and Tf-liposomal 5FU in HT-29 cells: A) ROS production, B) $\Delta\Psi_m$ collapse C) cytochrom c release, D) apoptosis and necrosis rate. Cells were exposed to the IC_{50} of free 5FU and Tf-liposomal 5FU for 48 h at 37 °C.
*Significant difference compared with control.
#Significant difference compared with free drug.

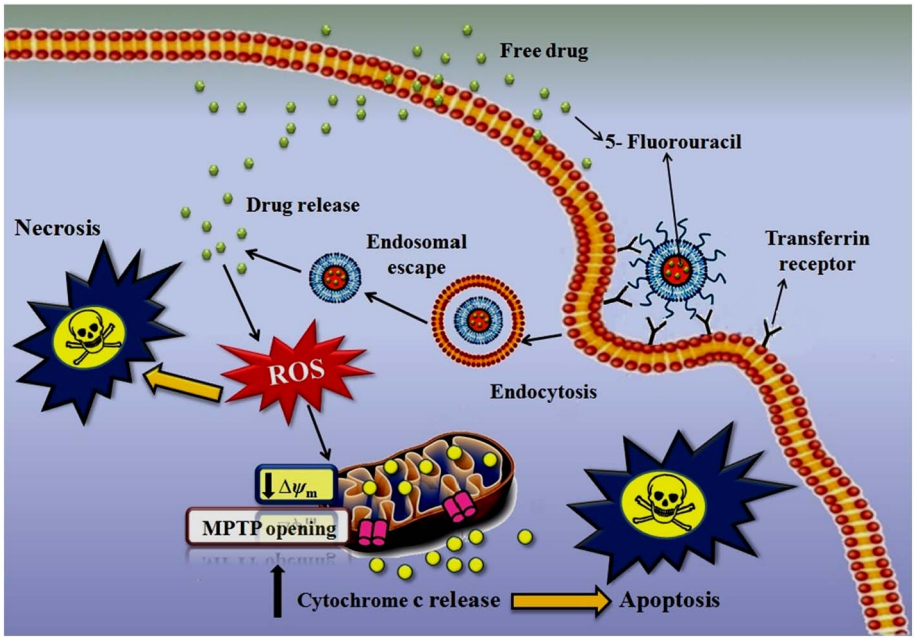

Fig. 6. Schematic illustration of mechanism of action of 5FU and Tf-liposomal 5FU.

which showed that Tf targeted doxorubicin induced more apoptosis than free doxorubicin in cancer cells [39]. Huang et al. found that Tf targeted selenium nano-particles trigged intracellular ROS over-production and promoted apoptosis pathway in cancer cells [31]. Dilnawaz et al. reported that Tf targeted nano-particles reduced $\Delta\psi_m$ more than nano-targeted nano-particles and free drug due to higher cellular uptake of the receptor conjugated drug-loaded nano-particles [40]. Previous study of Mulik et al. in this field is also accordant with these findings. They reported that Tf targeted curcumin-loaded SLN (Tf-C-SLN) induce ROS generation in breast cancer cells. The ROS production with Tf-C-SLN was extensively decreased with pre-addition of free Tf compared to Tf-C-SLN alone, demonstrating the Tf-receptor blocking on the cell surface and therefore, reduced uptake of Tf-C-SLN in the presence of free Tf. Consequently, cellular uptake of Tf targeted nano-particles was confirmed by Tf-mediated endocytosis [41]. The mechanism of action of 5FU and Tf-liposomal 5FU is presented in Fig. 6.

4. Conclusion

Transferrin targeted liposomal 5FU was developed to improve the safety and efficacy of the cytotoxic agent. The EE% of the liposomes was 58.66 ± 0.58 and their particle size was around 107 nm. According to the results of MTT, targeted liposomes improved cytotoxic activity of 5FU in comparison to free drug and non-targeted 5FU

containing liposomes with lower dose. Furthermore, Tf-liposomal 5FU induced apoptosis in cancer cells by lower production of ROS, decreased $\Delta\Psi_m$ and higher release of cytochrome *c*. It is concluded that Tf targeted liposomes would provide a promising therapeutic approach for cancer.

Conflict of interest

The authors do not have a direct financial relation with the commercial identities mentioned in our paper.

Acknowledgment

The work was financially supported by Nanotechnology Research Center, Ahvaz Jundishapur University of Medical Sciences, Ahvaz, Iran (grant No. 111) and Iran National Science Foundation (grant no. INSF-93032941). Also, the authors gratefully thank Dr. Azar Mostoufi and Dr. Masood Fereidoonnezhad for their cooperation in analyzing FT-IR spectra.

References

[1] S. Jaferian, B. Negahdari, A. Eatemadi, Colon cancer targeting using conjugates biomaterial 5-flurouracil, Biomed. Pharmacother. 84 (2016) 780–788.
[2] A.K. Yadav, A. Agarwal, G. Rai, P. Mishra, S. Jain, A.K. Mishra, H. Agrawal, G.P. Agrawal, Development and characterization of hyaluronic acid decorated PLGA nanoparticles for delivery of 5-fluorouracil, Drug Deliv. 17 (2010) 561–572.
[3] Y.S. Krishnaiah, V. Satyanarayana, B. Dinesh Kumar, R.S. Karthikeyan, P. Bhaskar, In vivo pharmacokinetics in human volunteers: oral administered guar gum-based colon-targeted 5-fluorouracil tablets, Eur. J. Pharm. Sci. 19 (2003) 355–362.
[4] A.C. Mattos, C. Altmeyer, T.T. Tominaga, N.M. Khalil, R.M. Mainardes, Polymeric nanoparticles for oral delivery of 5-fluorouracil: formulation optimization, cytotoxicity assay and pre-clinical pharmacokinetics study, Eur. J. Pharm. Sci. 84 (2016) 83–91.
[5] A. Sharma, A. Kaur, U.K. Jain, R. Chandra, J. Madan, Stealth recombinant human serum albumin nanoparticles conjugating 5-fluorouracil augmented drug delivery and cytotoxicity in human colon cancer, HT-29 cells, Colloids Surf. B: Biointerfaces 155 (2017) 200–208.
[6] A. Akbarzadeh, R. Rezaei-Sadabady, S. Davaran, S.W. Joo, N. Zarghami, Y. Hanifehpour, M. Samiei, M. Kouhi, K. Nejati-Koshki, Liposome: classification, preparation, and applications, Nanoscale Res. Lett. 8 (2013) 102.
[7] Y. Guo, L. Wang, P. Lv, P. Zhang, Transferrin-conjugated doxorubicin-loaded lipid-coated nanoparticles for the targeting and therapy of lung cancer, Oncol. Lett. 9 (2015) 1065–1072.
[8] S. Pereira, R. Egbu, G. Jannati, W.T. Al-Jamal, Docetaxel-loaded liposomes: the effect of lipid composition and purification on drug encapsulation and in vitro toxicity, Int. J. Pharm. 514 (2016) 150–159.
[9] M.M. Gaspar, A. Radomska, O.L. Gobbo, U. Bakowsky, M.W. Radomski, C. Ehrhardt, Targeted delivery of transferrin-conjugated liposomes to an orthotopic model of lung cancer in nude rats, J. Aerosol Med. Pulm. Drug Deliv. 25 (2012) 310–318.
[10] R. Wang, H. Cui, J. Wang, N. Li, Q. Zhao, Y. Zhou, Z. Lv, W. Zhong, Enhancing the antitumor effect of methotrexate in intro and in vivo by a novel targeted single-walled carbon nanohorn-based drug delivery system, RSC Adv. 6 (2016) 47272–47280.
[11] X. Li, L. Ding, Y. Xu, Y. Wang, Q. Ping, Targeted delivery of doxorubicin using stealth liposomes modified with transferrin, Int. J. Pharm. 373 (2009) 116–123.
[12] P.P. Deshpande, S. Biswas, V.P. Torchilin, Current trends in the use of liposomes for tumor targeting, Nanomedicine 8 (2013) 1509–1528.
[13] Z. Su, Z. Yang, Y. Xu, Y. Chen, Q. Yu, Apoptosis, autophagy, necroptosis, and cancer metastasis, Mol. Cancer 14 (2015) 48.
[14] M.G. Baigi, L. Brault, A. Néguesque, M. Beley, R.E. Hilali, F. Gaüzère, D. Bagrel, Apoptosis/necrosis switch in two different cancer cell lines: influence of benzoquinone- and hydrogen peroxide-induced oxidative stress intensity, and glutathione, Toxicol. in Vitro 22 (2008) 1547–1554.
[15] M. Higuchi, T. Honda, R.J. Proske, E.T. Yeh, Regulation of reactive oxygen species-induced apoptosis and necrosis by caspase 3-like proteases, Oncogene 17 (1998) 2753–2760.
[16] A. Waheed, Y. Bibi, S. Nisa, F.M. Chaudhary, S. Sahreen, M. Zia, Inhibition of human breast and colorectal cancer cells by *Viburnum foetens* L. extracts in vitro, Asian Pac. J. Trop. Dis. 3 (2013) 32–36.
[17] R.J. Lee, P.S. Low, Folate-mediated tumor cell targeting of liposome-entrapped doxorubicin in vitro, Biochim. Biophys. Acta 1233 (1995) 134–144.
[18] H. Wang, J.A. Joseph, Quantifying cellular oxidative stress by dichlorofluorescein assay using microplate reader, Free Radic. Biol. Med. 27 (1999) 612–616.
[19] B. Elorza, M.A. Elorza, G. Frutos, J.R. Chantres, Characterization of 5-fluorouracil loaded liposomes prepared by reverse-phase evaporation or freezing-thawing extrusion methods: study of drug release, Biochim. Biophys. Acta 1153 (1993) 135–142.
[20] M. Glavas-Dodov, E. Fredro-Kumbaradzi, K. Goracinova, M. Simonoska, S. Calis, S. Trajkovic-Jolevska, A.A. Hincal, The effects of lyophilization on the stability of liposomes containing 5-FU, Int. J. Pharm. 291 (2005) 79–86.
[21] A.N. Elmeshad, S.M. Mortazavi, M.R. Mozafari, Formulation and characterization of nanoliposomal 5-fluorouracil for cancer nanotherapy, J. Liposome Res. 24 (2014) 1–9.
[22] N. Kaiser, A. Kimpfler, U. Massing, A.M. Burger, H.H. Fiebig, M. Brandl, R. Schubert, 5-Fluorouracil in vesicular phospholipid gels for anticancer treatment: entrapment and release properties, Int. J. Pharm. 256 (2003) 123–131.
[23] T. Shigehiro, T. Kasai, M. Murakami, S.C. Sekhar, Y. Tominaga, M. Okada, T. Kudoh, A. Mizutani, H. Murakami, D.S. Salomon, K. Mikuni, T. Mandai, H. Hamada, M. Seno, Efficient drug delivery of Paclitaxel glycoside: a novel solubility gradient encapsulation into liposomes coupled with immunoliposomes preparation, PLoS One 9 (2014) e107976.
[24] B. Xiao, M.K. Han, E. Viennois, L. Wang, M. Zhang, X. Si, D. Merlin, Hyaluronic acid-functionalized polymeric nanoparticles for colon cancer-targeted combination chemotherapy, Nano 7 (2015) 17745–17755.
[25] Y. Sun, Z.L. Sun, Transferrin-conjugated polymeric nanomedicine to enhance the anticancer efficacy of edelfosine in acute myeloid leukemia, Biomed. Pharmacother. 83 (2016) 51–57.
[26] H. Zhang, L. Hou, X. Jiao, Y. Ji, X. Zhu, Z. Zhang, Transferrin-mediated fullerenes nanoparticles as Fe^{2+}-dependent drug vehicles for synergistic anti-tumor efficacy, Biomaterials 37 (2015) 353–366.
[27] R.P. Singh, G. Sharma, Sonali, P. Agrawal, B.L. Pandey, B. Koch, M.S. Muthu, Transferrin receptor targeted PLA-TPGS micelles improved efficacy and safety in docetaxel delivery, Int. J. Biol. Macromol. 83 (2016) 335–344.
[28] M. Kawamoto, T. Horibe, M. Kohno, K. Kawakami, A novel transferrin receptor-targeted hybrid peptide disintegrates cancer cell membrane to induce rapid killing of cancer cells, BMC Cancer 11 (2011) 359–371.
[29] R. Gerl, D.L. Vaux, Apoptosis in the development and treatment of cancer, Carcinogenesis 26 (2005) 263–270.
[30] T.-H. Kim, G.-W. Jeong, J.-W. Nah, Preparation and anticancer effect of transferrin-modified pH-sensitive polymeric drug nanoparticle for targeted cancer therapy, J. Ind. Eng. Chem.
[31] Y. Huang, L. He, W. Liu, C. Fan, W. Zheng, Y.S. Wong, T. Chen, Selective cellular uptake and induction of apoptosis of cancer-targeted selenium nanoparticles, Biomaterials 34 (2013) 7106–7116.
[32] Y. Sun, B. Rigas, The thioredoxin system mediates redox-induced cell death in human colon cancer cells: implications for the mechanism of action of anticancer agents, Cancer Res. 68 (2008) 8269–8277.
[33] I.T. Hwang, Y.M. Chung, J.J. Kim, J.S. Chung, B.S. Kim, H.J. Kim, J.S. Kim, Y.D. Yoo, Drug resistance to 5-FU linked to reactive oxygen species modulator 1, Biochem. Biophys. Res. Commun. 359 (2007) 304–310.
[34] D.F. Stowe, A.K. Camara, Mitochondrial reactive oxygen species production in excitable cells: modulators of mitochondrial and cell function, Antioxid. Redox Signal. 11 (2009) 1373–1414.
[35] C. Guo, L. Sun, X. Chen, D. Zhang, Oxidative stress, mitochondrial damage and neurodegenerative diseases, Neural Regen. Res. 8 (2013) 2003–2014.
[36] L. Sliwka, K. Wiktorska, P. Suchocki, M. Milczarek, S. Mielczarek, K. Lubelska, T. Cierpial, P. Lyzwa, P. Kielbasinski, A. Jaromin, A. Flis, Z. Chilmonczyk, The comparison of MTT and CVS assays for the assessment of anticancer agent interactions, PLoS One 11 (2016) e0155772.
[37] B. Shen, P.-J. He, C.-L. Shao, Norcantharidin induced DU145 cell apoptosis through ROS-mediated mitochondrial dysfunction and energy depletion, PLoS One 8 (2013) e84610.
[38] T. Iba, N. Hashiguchi, I. Nagaoka, Y. Tabe, M. Murai, Neutrophil cell death in response to infection and its relation to coagulation, J. Intensive Care 1 (2013) 13.
[39] M. Szwed, A. Laroche-Clary, J. Robert, Z. Jozwiak, Induction of apoptosis by doxorubicin-transferrin conjugate compared to free doxorubicin in the human leukemia cell lines, Chem. Biol. Interact. 220 (2014) 140–148.
[40] F. Dilnawaz, A. Singh, S.K. Sahoo, Transferrin-conjugated curcumin-loaded superparamagnetic iron oxide nanoparticles induce augmented cellular uptake and apoptosis in K562 cells, Acta Biomater. 8 (2012) 704–719.
[41] R.S. Mulik, J. Monkkonen, R.O. Juvonen, K.R. Mahadik, A.R. Paradkar, Transferrin mediated solid lipid nanoparticles containing curcumin: enhanced in vitro anticancer activity by induction of apoptosis, Int. J. Pharm. 398 (2010) 190–203.